# PRELIMINARY MODELING OF GRAPHITE DIVERTOR GEOMETRY EFFECTS ON THE STEADY STATE OPERATION OF THE PST TOKAMAK USING SOLPS 5.0

RAFAQAT ALI*, MUHAMMAD BILAL, KAMRAN AHMAD, SAIRA GULFAM, ZAHOOR AHMAD
Pakistan Tokamak Plasma Research Institute
Islamabad 44000, Pakistan
*rafaqat_ali3@hotmail.com

LIU XIAOJU
Institute of Plasma Physics Chinese Academy of Sciences
Hefei, Anhui, China
Email: julie1982@ipp.ac.cn

**Abstract**

Promising diverter shape for the steady state tokamak operation is optimized using different simulation codes. Optimization of diverter geometry and edge boundary conditions are necessary to access the high-density operating regimes, fusion ash removal and particle control scenarios. Pakistan Spherical Tokamak (PST-I) is a medium sized spherical tokamak in design phase. Double null divertor configuration is considered for the PST-I operation condition. This study focuses on the geometrical optimization of the graphite double null divertor for PST-1. Two different divertor geometries (A & B) are considered in this study. Maximum peak power for geometry A as measured by SOLPS 5.0 code is 12 MW and for geometry B peak power is 6 MW at the lower outer target which is 2 times lower than the geometry A. Similarly peak electron temperature for geometry A is 200 eV and for geometry B is 120 eV for the input power of 0.8 MW.

## 1. INTRODUCTION

Fusion is environment friendly and long-lasting source of energy for the future mankind needs. Among many engineering and physics restrictions, high heat and particle flux reaching the plasma facing components (PFCs) [1] and causing the sputtering/erosion of first wall material is the major restriction. These sputtered plasma particles can deteriorate plasma performance. The divertor and limiter parts are subjected to these high heat and particle fluxes. Among many in vessel components, divertor is the critical part of the tokamak device. It performs the following important functions;

- It is used to extract heat and particle fluence
- It extracts helium ash and impurities from the tokamak device
- It also improves plasma performance by providing better control on plasma density

Diverter geometry also affects the peak power load and ionization control, divertor radiation power loss, deuterium and impurity pumping, neutral particle pressure control and plasma confinement [2]. Diverter geometrical parameters are optimized by the use of different codes like PFCFlux [3], UEDGE, SOLPS [4], SOLPS-ITER, EDGE2D [5] and SOLEDGE2D [6].

In physics design phase of graphite double null diverter of PST-I, electron temperature, electron density, heat flux on the mid plane and diverter target are focused with respect to the diverter geometry. Further the scrap off layer width is also calculated using the SOLPS fittings.

## 2. CODE

SOLPS 5.0 (Scrape-Off Layer Simulation) code is used in present study. SOLPS is combination of B2.5 2D code and EIRENE-3D Monte-carlo code. B2.5 2D is used for the transport of charged particles. EIRENE-3D Monte-carlo code is used for the transport of the neutrals.

Different input parameters required for the SOLPS code are as follow;

- Magnetic configuration (gfile of the EFIT)
- Coordinates of the first wall
- Core electron temperature
- Core plasma density
- Plasma current
- Input power (ohmic + auxiliary)
- Number of the exhaust ports

- Pumping speed of the pumping station

## 3. GEOMETRY

Two geometries are selected for the physics design study of the divertor. Figure 1a is showing the upper and lower divertor geometry A. It consists of inner and outer vertical plates and a central horizontal dome plate. Flat plate for both upper and lower outer divertor targets are considered. Vertical plate for both upper and lower inner divertor targets are selected.

In geometry B oblique plates for both upper and lower outer divertor targets are considered as shown in the Figure 1b. These geometries have the following advantages

- Easy to manufacture and install
- Save the cost
- Flexible to be compatible with different magnetic configurations

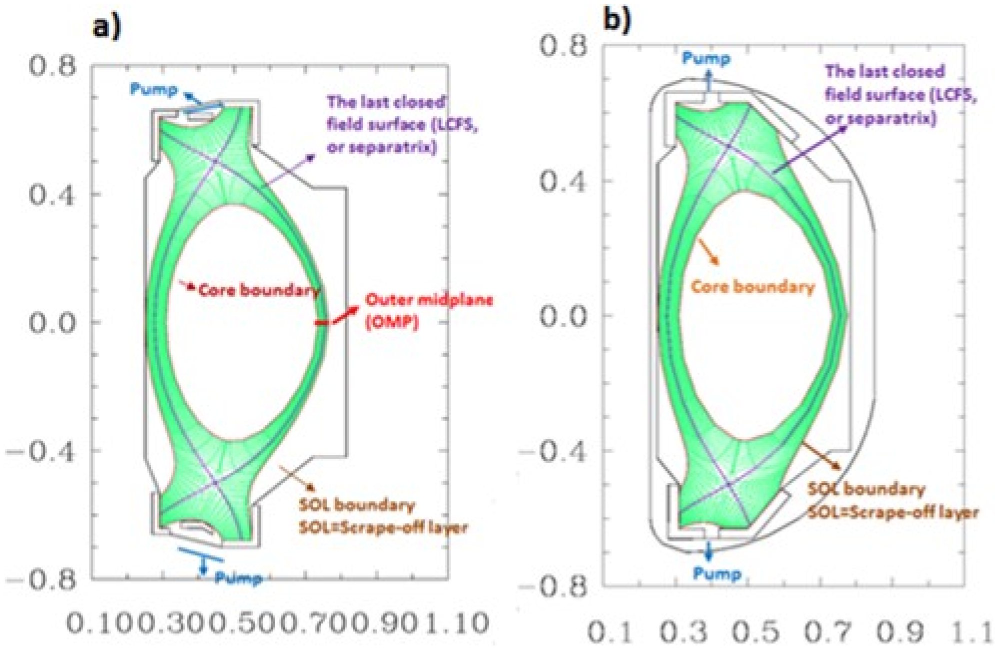


*FIG. 1. a) Divertor geometry A* *b) Divertor geometry B.*

## 4. BOUNDARY CONDITIONS

Particle transport coefficient D = 0.3$m^2$/s and heat transport coefficient $\chi_{i/e}$ = 1.0 $m^2$/s is used in this study. Graphite material is used for the divertor target and the physical and chemical sputtering of graphite are considered. The chemical sputtering yield of 2% is considered. Pumping port is chosen under the dome. Pump speed of S ~ 34 ($m^3$/s) is used in the code.

$$\text{Pump speed} = S \approx A(1-R)\times 36.38\times\sqrt{T/m}$$

Where A is surface area ($m^2$), R is recycling rate, T is temperature (K), usually assume ~300K (room temperature) and **m** is mass (AMU), 2 for D. Pump speed can by changed by modifying R on the pump slot surface. In this simulation no drift effects are considered.

## 5. POWER EXHAUST LEVEL

Input power in a tokamak consists of ohmic power and auxiliary heating power, while 70-80% of this input power is transferred in separatrix.

$$P_{in} = P_{oh} + P_{aux}, \qquad P_{sep} \cong 80\%\ P_{in}$$

While 20% $P_{in}$ is radiated inside core boundary. Power handling coefficient - $P_{sep}/R$ is comparable to that of EAST.

## 6. CORE BOUNDARY

We considered three different values of separatrix heat flux

$$\text{Power, } P_{sep} = P_e + P_i = 400/600/800 \text{ kW}, \qquad P_e = P_i = 200/300/400 \text{ kW}$$

Similarly, three different separatrix ion densities are considered.

$$n_{sep} = 0.7/0.9/1.0/1.2/1.5 \times 10^{19}\ m^{-3}$$

## 7. RESULTS AND DISCUSSION

As the input power calculated from physics design, is not the absorption power so there was need to scan the data for different powers. Similarly core plasma density was provided by the physics design so there was need to scan the data for the different edge plasma densities. Absorbed power values selected for the simulation were 0.4, 0.6 and 0.8 MW. Different values of the edge plasma density used for the simulations are 0.5, 0.7, 0.9 and 1 ($10^{19}/m^3$)

## 8. MID-PLANE

Code was run for the different input powers and edge plasma density to check the effect of these variables on the electron temperature, plasma density and the heat flux on the target.

Figure 2 shows the electron temperature and the density variation along the mid plane for the different selected edge plasma densities at input power of 0.4 MW. It is clear from the Figure 2 that for the lower edge plasma density the value of the electron temperature is higher and continue to decrease towards the edge plasma. Similarly with the increase in edge plasma density, an increase in core plasma density is observed.

Figure 3 is plotted for electron temperature and the density variation along the mid plane for the different selected edge plasma densities with input power of 0.6 MW. Figure shows that for the lower edge plasma density the value of the electron temperature (650 eV) is higher and continue to decrease towards the edge plasma. Similarly with the increase in edge plasma density, an increase in core plasma density (2.6) is observed.

Figure 4 shows the electron temperature and the density variation along the mid plane for the different selected edge plasma densities at input power of 0.8 MW. A similar trend is observed for the lower edge plasma density with electron temperature (800 eV).

## 9. DIVERTOR TARGET

Figure 5 shows the variation in the electron temperature and power density on the lower inner and outer divertor target plates for the input power of 0.4 MW and different edge plasma densities. For the lower edge plasma density higher electron temperature was observed. Te at lower outer target for ne = 0.5 is 110 eV and for ne = 1 the value of Te is 55eV. Similarly, power density at the lower outer target plate is 5 $MW/m^2$ and at lower inner target is 3 $MW/m^2$. There is no much variation in power density with the change in edge plasma density as it is clear from figure 5a.

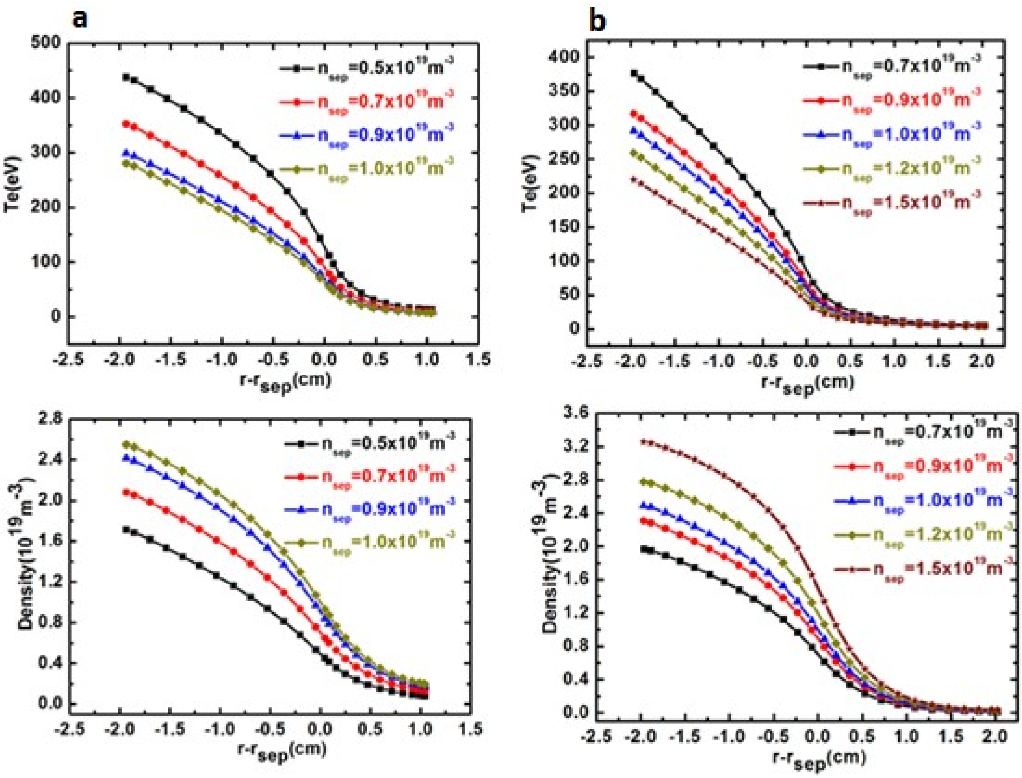


*FIG. 2. Electron temperature and density variation for input power of 400 kW at mid plane for a) geometry A b) geometry B.*

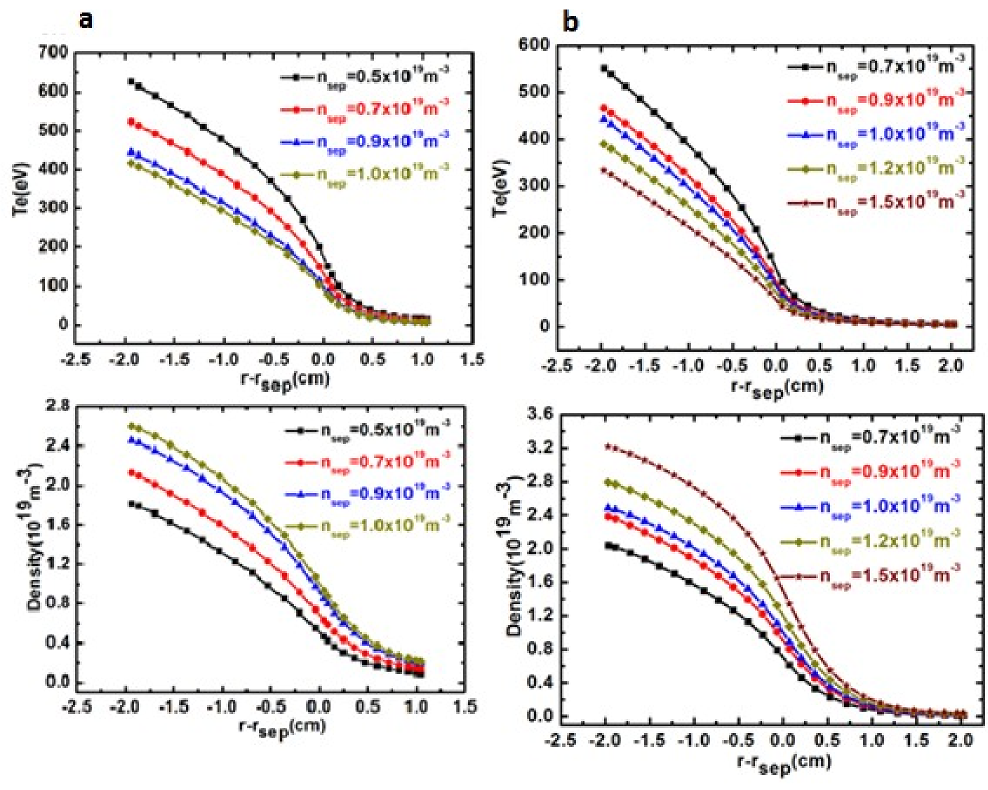


*FIG. 3. Electron temperature and density variation for input power of 600 kW at mid plane for a) geometry A b) geometry B.*

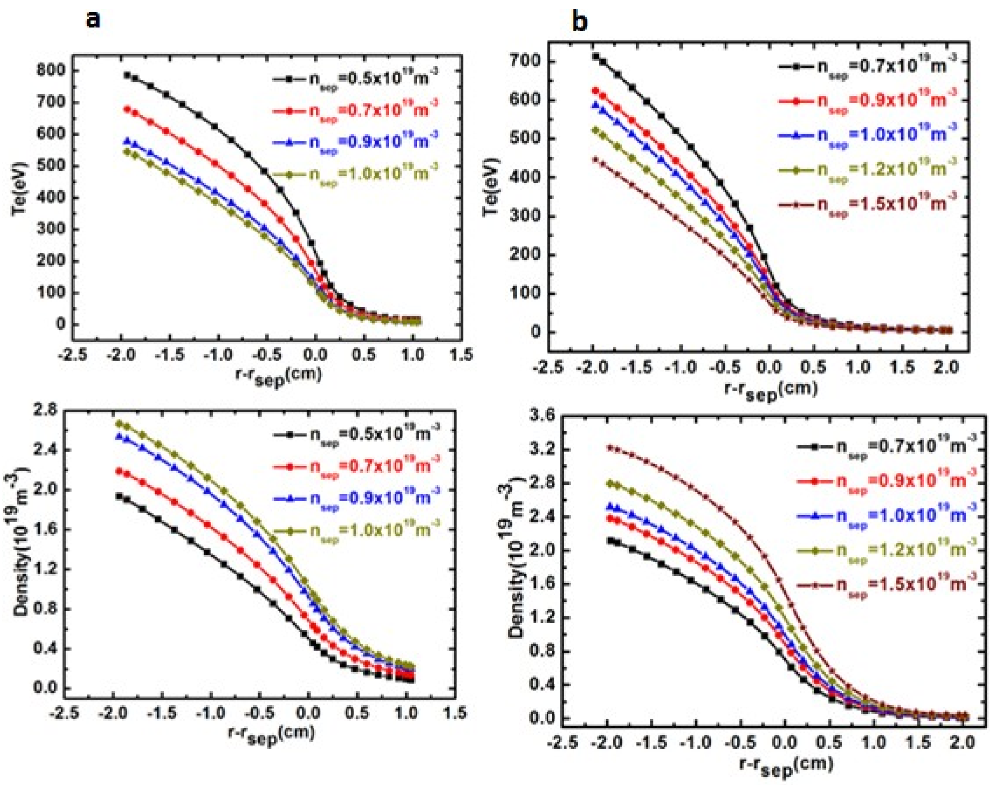


*FIG. 4. Electron temperature and density variation for input power of 800 kW at mid plane for a) geometry A b) geometry B.*

Figure 6 shows the variation in the electron temperature and power density on the lower inner and outer target plate for the input power of 0.6 MW and different edge plasma densities. For the lower edge plasma density higher electron temperature was observed. Te at lower outer target for ne = 0.5 is 150 eV and for ne = 1 the value of Te is 80eV. Similarly, Te at lower inner target plate is 85 eV for ne =0.5 and 40 eV for ne = 1. Similarly for different edge plasma densities value of the power density at the lower outer target plate is 8 $MW/m^2$ and at lower inner target is 4.5 $MW/m^2$ as can be seen in the figure 6a.

Figure 7 shows the variation in the electron temperature and power density on the lower inner and outer target plate for the input power of 0.8 MW and different edge plasma densities. For the lower edge plasma density higher electron temperature was observed at both outer and inner target. Te at lower outer target for ne = 0.5 is 190 eV and for ne = 1 the value of Te is 100eV. Similarly, Te at lower inner target plate is 85 eV for ne =0.5 and 60 eV for ne = 1. Similarly for different edge plasma densities value of the power density at the lower outer target plate is 12 $MW/m^2$ and at lower inner target is 6 $MW/m^2$ as can be seen in the figure 7a.

## 10. PEAK ELECTRON TEMPERATURE AND POWER LOAD ON LOWER TARGET

Figure 8a shows the peak electron temperature and heat flux for different values of the separatrix density, power for geometry A. $T_{e\text{-peak}}$ decreases with the increase in $n_{sep}$ however little change in the peak power flux is observed with the increase in separatrix density. It means that separatrix density has little effect on the peak power flux. Peak electron temperature and power flux observed is 190 eV and 12 MW/m2 for input power of 0.8 MW. For geometry A as the input power is increased electron temperature and the peak power flux on the lower target is increased as is seen from the figure 8a.

Figure 8b shows the peak electron temperature and heat flux for different values of the separatrix density and power for geometry B. Similar trend in $T_{e\text{-peak}}$ and peak power flux is observed in geometry B with the increase in separatrix density. As the input power is increased electron temperature and the peak power flux on the lower target is increased as is seen from the figure 8b. Peak electron temperature and power flux observed for geometry B, is 120 eV and 6 $MW/m^2$ for input power of 0.8 MW. Decrease in peak electron temperature and power flux is observed in the modelling of geometry B. These values of peak electron temperature and power flux are still higher. So different geometry scan will be considered in future work.

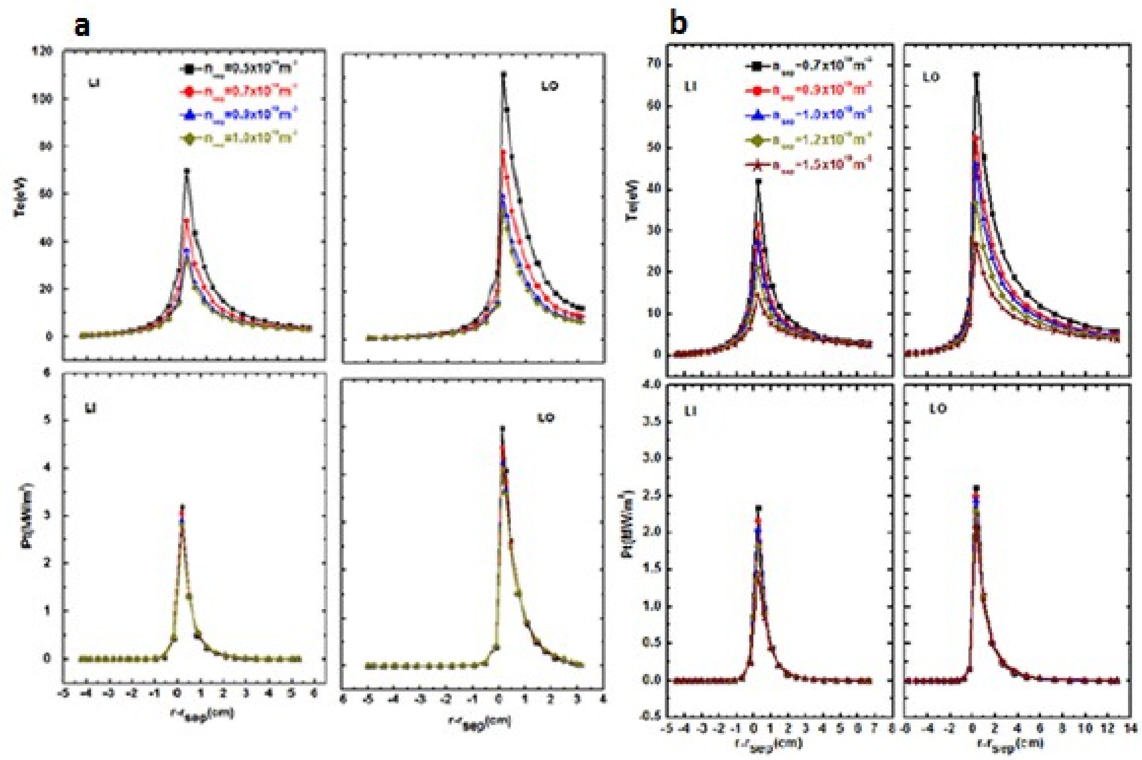


*FIG. 5. Electron temperature and heat flux variation for input power of 400 kW at lower inner and outer divertor target for a) geometry A b) geometry B.*

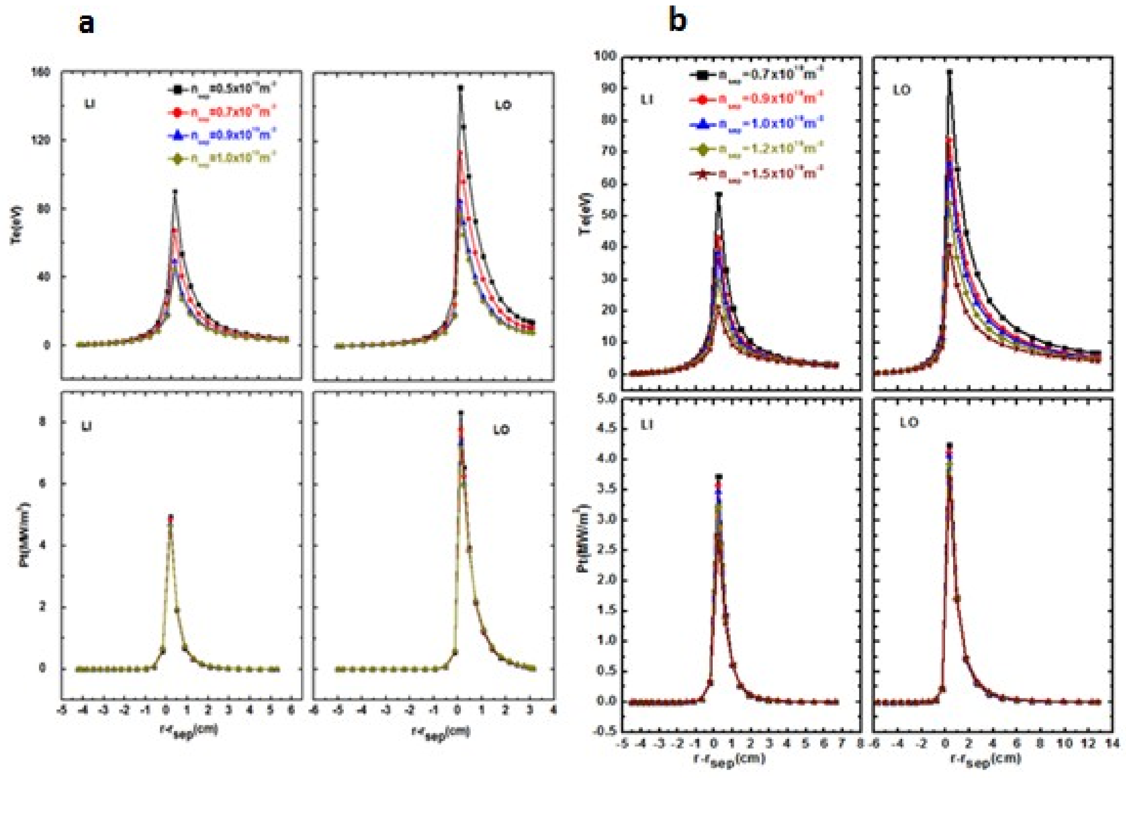


*FIG. 6. Electron temperature and heat flux variation for input power of 600 kW at lower inner and outer divertor target for a) geometry A b) geometry B.*

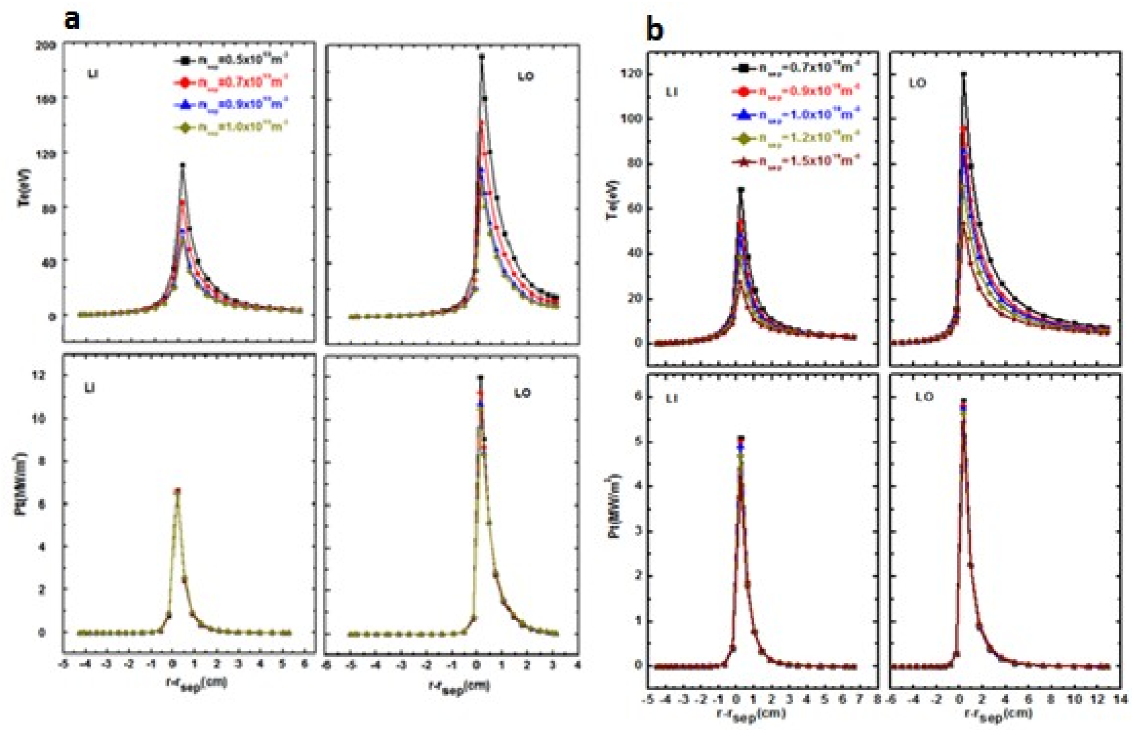


*FIG. 7. Electron temperature and heat flux variation for input power of 800 kW at lower inner and outer divertor target for a) geometry A b) geometry B.*

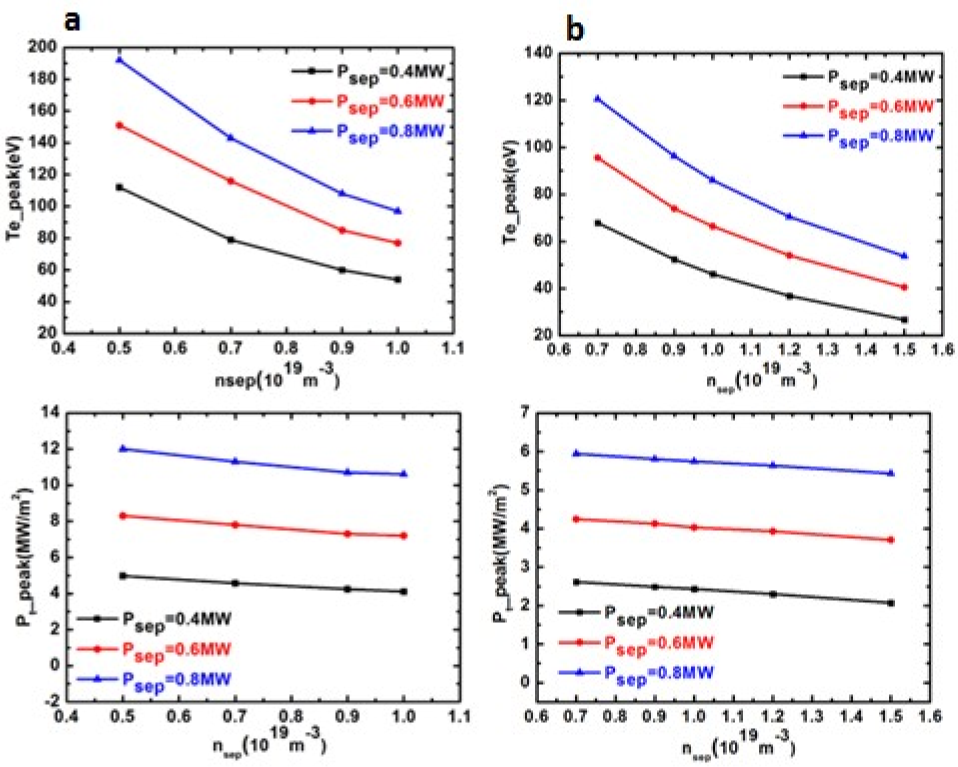


*FIG. 8. Peak electron temperature and power load on lower target of a) Geometry A b) Geometry B.*

## 11. POWER DECAY LENGTH

Power decay length is important variable which governs the dynamics of power exhaust. It also affects the plasma detachment scenarios. For the separatrix power load $P_{sep}$=0.6MW and separatrix flux density $n_{sep}=1.0\times10^{19}m^{-3}$ the power decay length $\lambda_q$ fitted from SOLPS is about 8mm.

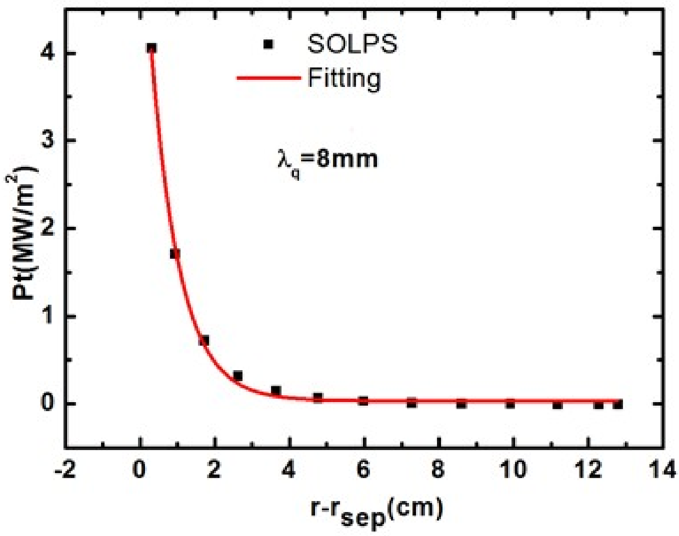


*FIG. 9. Scrap of layer (SOL) width.*

## 12. CONCLUSIONS

A preliminary double null divertor of PST-1 has been designed with two outer flat target plates and two inner vertical target plates. The heat load on divertor targets is very high due to the small wetted area on divertor target plates. Continuous optimization on divertor design is needed. Peak electron temperature is 200 eV for geometry A and 120 eV for geometry B. Similarly for geometry A peak heat load is 12 MW and for geometry B peak heat load is 6 MW. Power decay length measured from SOLPS fitting is 8 mm for the separatrix power load of 0.6MW and separatrix flux density of $1.0\times10^{19}m^{-3}$.

## REFERENCES

[1] MARENKOV, E., PSHENOV, A., Vapor shielding of liquid lithium divertor target during steady-state and transient events, Nuclear Fusion **60** 2 (2020) 026011.

[2] LOARTE, A., Effects of divertor geometry on tokamak plasmas, Plasma Physics and Controlled Fusion, **43** 6 (2001) R183.

[3] ZHANG, B., FIRDAOUSS, M., GONG, X., EKEDAHL, A., PENG, X., ZHANG, X., Study of power load pattern on EAST divertor using PFCFlux code, Fusion Engineering and Design, **107** (2016) 58–63.

[4] CANIK, J. M., MAINGI, R., OWEN, L., MENARD, J., GOLDSTON, R., KOTSCHENREUTHER, M., VALANJU, P., MAHAJAN, S., 2D divertor design calculations for the national high-power advanced torus experiment, Journal of nuclear materials **390** (2009) 315-318.

[5] RUBINO, G., AMBROSINO, R., CALABRÒ, G., RIDOLFINI, V. P., VIOLA, B., Comparative analysis of the SOL plasma in DEMO using EDGE2D/EIRENE and TECXY codes, Nuclear Materials and Energy **12** (2017) 864-868.

[6] JESKO, K., Y. MARANDET, H. BUFFERAND, J. P. GUNN, H. J. VAN DER MEIDEN, AND G. CIRAOLO, Soledge2D-Eirene simulations of the Pilot-PSI linear plasma device compared to experimental data, Contributions to Plasma Physics, **58** 6–8 (2018) 798–804.